

---

---

## SPECTROSCOPY OF ATOMS AND MOLECULES

---

---

# Development of Multiple-Wavelength Oscillation in Plasma of a Pulse-Periodic He + Ne + Sr Laser

T. M. Gorbunova, A. N. Soldatov, Yu. P. Polunin, and A. V. Lugovskoi

*National Research Tomsk State University, Tomsk, 634036 Russia*

*e-mail: general@tic.tsu.ru*

Received May 8, 2014

**Abstract**—Mechanisms of multiple-wavelength oscillation at the lines of He I, Ne I, Sr I, and Sr II ions in the active medium of a high-voltage pulse-periodic laser based on a He + Ne + Sr mixture at a total pressure of ~200 Torr and duration of the current pulse of about 150–300 ns are analyzed. An important role played by collisional thermal mixing of the laser levels of Ne I and Sr I in multiplets, as well as by collisions of the second kind between metastable and unexcited atoms, in populating and depopulating atomic levels is demonstrated. Absolute populations of the upper and lower levels of the laser transitions in Ne I are found. It is discovered that the degree of ionization nonequilibrium of plasma, both during and after the pulse of current, determines the mechanism of population inversion in laser transitions.

**DOI:** 10.1134/S0030400X15030145

### INTRODUCTION

High-voltage longitudinally pumped pulse-periodic metal vapor lasers based on He(Ne) + Sr, He + Ne + Sr mixtures with buffer gas pressure of 30–200 Torr and strontium vapor pressure of 0.1–2 Torr are primarily known with regard to their oscillation at the Sr I line with wavelength  $\lambda = 6.456 \mu\text{m}$ . This kind of laser oscillation takes place in lasers based on self-limited transitions from the resonance level to the metastable one (the so-called  $r$ – $m$  transitions). In this case, the maximum average laser power approaches 20 W. Under comparable excitation conditions, laser emission at  $r$ – $m$  transitions of Sr II with wavelengths  $\lambda = 1.03$  and  $1.09 \mu\text{m}$ , along with laser emission at transition of He I with wavelength  $\lambda = 2.06 \mu\text{m}$ , have also been observed [1, 2].

As a rule, lasers based on  $r$ – $m$  transitions operate in accordance with the longitudinal electric discharge scheme, although the efficiency of transverse-discharge pumping is substantially higher. In the longitudinal discharge scheme, the average electric field in the discharge volume is much lower than that in the transverse discharge scheme and pumping is less efficient, because the rate of the gas excitation and ionization exponentially depends on  $E/p$ . Since the beam quality of transversely pumped lasers is inadequate for many technical and scientific applications, longitudinally pumped lasers are used instead [3]. The high-voltage discharges with the longitudinal excitation studied in the present work are stable systems with respect to the construction of the gas-discharge source, the method of formation of the nano-

second voltage pulses, and the character of variation of current, in which strongly nonequilibrium plasma is created by the simultaneous action of an electron beam and an electric discharge. In such systems, the high-speed ionization waves (HSIW) leading to filling of the discharge gap by highly ionized plasma at a sublight velocity and characterized by the presence of strong electric fields and high-energy (runaway) electrons in their front are created in the vicinity of the high-voltage electrode (the cathode in our case) [3, 4].

Diagnostics of plasma conducted in [5] revealed that the discharge in a He(Ne) + Sr mixture under the above-specified values of the pressure and the high-voltage pulse amplitude of ~10 kV takes the form of a discharge sliding along the dielectric surface of the gas-discharge tube (GDT). In so doing, the longitudinal HSIW leaves a substantial charge on the surface of the dielectric, which, in turn, creates a transverse electric field pushing plasma toward the GDT center. The plasma column characterized by high electron temperature  $T_e$  and concentration  $n_e$  forms at considerable distance from the walls and moves toward the center, with the speed of this motion being higher in helium than in neon. To prevent overheating in the tube center, neon was added to helium, which resulted in the onset of oscillation around a group of transitions of Ne I emitting radiation at ~1  $\mu\text{m}$ , at the He I line with wavelength  $\lambda = 2.06 \mu\text{m}$ , as well as at two lines of Ne I in the visible spectral range [1, 6].

Laser lines, transitions corresponding to them, energies of the upper and lower states, and their notation

No.	Radiation wavelength, nm	$E_u$ , eV	$E_l$ , eV	Transitions in $L-S$ coupling notations	Transitions in Racah* notations	Transitions in Paschen notations
1	1029.5 NeI	19.78	18.58	$4s^1P_1-3p^3D_2$	$4s'[1/2]_1^\circ-3p[5/2]_2$	$2s_2-2p_8$
2	1033.0 Sr II	3.04	1.81	$5p^2P_{3/2}^\circ-4d^2D_{5/2}$		
3	1079.8 NeI	19.78	18.61	$4s^1P_1-3p^3D_1$	$4s'[1/2]_1^\circ-3p[3/2]_1$	$2s_2-2p_7$
4	1084.4 NeI	19.78	18.64	$4s^1P_1-3p^1D_2$	$4s'[1/2]_1^\circ-3p[3/2]_2$	$2s_2-2p_6$
5	1091.4 Sr II	2.96	1.84	$5p^2P_{3/2}^\circ-4d^2D_{3/2}$		
6	1117.7 NeI	19.66	18.56	$4s^3P_2-3p^3D_3$	$4s[3/2]_2^\circ-3p[5/2]_3$	$2s_5-2p_9$
7	1152.3 NeI	19.78	18.69	$4s^1P_1-3p^3P_2$	$4s'[1/2]_1^\circ-3p'[3/2]_1$	$2s_2-2p_4$
8	1176.7 NeI	19.78	18.73	$4s^1P_1-3p^3P_1$	$4s'[1/2]_1^\circ-3p'[1/2]_1$	$2s_2-2p_2$
9	1259.4 NeI	19.69	18.69	$4s^3P_1-3p^3P_1$	$4s[3/2]_1^\circ-3p'[3/2]_1$	$2s_4-2p_4$
10	1268.9 NeI	19.69	18.7	$4s^3P_1-3p^3P_0$	$4s[3/2]_1^\circ-3p[1/2]_0$	$2s_4-2p_3$
11	1288.7 NeI	19.69	18.73	$4s^3P_1-3p^3P_1$	$4s[3/2]_1^\circ-3p'[1/2]_1$	$2s_4-2p_2$
12	1523.1 NeI	19.78	18.97	$4s^1P_1-3p^1S_0$	$4s'[1/2]_1^\circ-3p'[1/2]_0$	$2s_2-2p_1$
13	2058.1 He I	21.22	20.62	$2p^1P_1-2s^1S_0$		
14	2691.5 Sr I	2.26	1.8	$4d^3D_2-5p^3P_1^\circ$		
15	2922.5 Sr I	2.27	1.85	$4d^3D_3-5p^3P_1^\circ$		
16	3011.0 Sr I	2.26	1.85	$4d^3D_2-5p^3P_1^\circ$		
17	6456.0 Sr I	2.69	2.5	$5p^1P_1^\circ-4d^1D_2$		
18	585.3 NeI	18.97	16.85	$3p^1S_0-3s^1P_1$	$3p'[1/2]_0-3s'[1/2]_1^\circ$	$2p_1-1s_2$
19	540.1 NeI	18.97	16.67	$3p^1S_0-3s^3P_1$	$3p'[1/2]_0-3s[3/2]_1^\circ$	$2p_1-1s_4$

\* Primed and nonprimed levels in the sixth column correspond to different core states:  $nl = 2p^5(^2P_{3/2}^\circ)$ ,  $nl' = 2p^5(^2P_{1/2}^\circ)$ .

### EXPERIMENT IN A He + Ne + Sr MIXTURE

The first observation of the nearly simultaneous multiple-wavelength oscillation in a mixture of He I, Ne I, Sr I, Sr II atoms was reported in [2]. The studies were conducted with a gas-discharge source of laser radiation [5] the discharge channel of which was formed by a 50-cm-long BeO ceramic tube with an inner diameter of 2 cm. The active medium was pumped according to the scheme with a direct-discharge capacitor bank (~1175–1570 pF). A TGI-1000/25 thyatron was used as a commutator. The pulses of current, voltage, and laser oscillation were detected by means of a Rogowski coil, a P6015A voltage divider, and coaxial photocells, respectively. The signals detected by the sensors were fed into a Tektro-

nix TDS-3032 oscilloscope. The average power was monitored by an OPHIR (Nova II) power meter. The laser spectrum was studied by means of an MDR-204 monochromator with a spectral range extending up to ~5  $\mu\text{m}$ . Therefore, the Sr line at 6.45  $\mu\text{m}$  could not be detected. The active medium was pumped at a pulse repetition rate of 17–24 kHz and rectifier voltage of 3–5.5 kV. Any variation of frequencies and voltages caused changes in the steady-state thermal regime of the GDT. As a result, the amount of strontium vapors arriving into the discharge ( $P_{\text{Sr}}$  varied between 1 and 2.5 Torr). The relation between the intensities of the observed lines of oscillation, which are listed in the table, varied depending on the amount of strontium vapors in the discharge. At a maximal voltage (Fig. 1), laser emission lines of not only Sr I and Sr II, but also

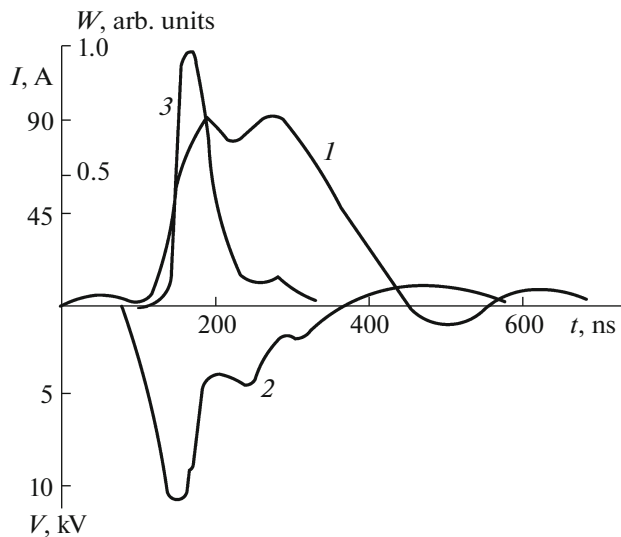


**Fig. 1.** (1) Pulse of current flowing through the GDT, (2) voltage across the GDT, and (3) laser oscillation pulse.

of He I and Ne I were observed. The onset of oscillation at all transitions, except those corresponding to  $\lambda = 0.5853$  and  $0.5401 \mu\text{m}$  and belonging to Ne I, took place at a steep front of the current pulse following the peak of the voltage pulse (Fig. 1). Oscillation at these two transitions was experimentally observed on the screen of the oscilloscope at the end of the current pulse, as well as visually. As an example, in Fig. 1, we present the time dependence of oscillation at Sr II transitions with emission wavelengths  $\lambda = 1.03$  and  $1.09 \mu\text{m}$  that were selected with a filter. Investigation of the He–Sr laser (without adding neon) revealed that oscillation in such laser occurs only at transitions of Sr atoms and ions [1]. Oscillation at the  $r$ – $m$  transition of He I corresponding to the laser emission with a wavelength of  $\lambda = 2.06 \mu\text{m}$  was appearing only after the introduction of neon into the He + Sr mixture with the ratio  $P_{\text{Ne}} : P_{\text{He}} \sim 1 : 2$  at a total gas pressure of  $\sim 200$  Torr. Vapors of strontium were introduced into the discharge upon heating of the GDT discharge channel walls to temperatures in the range between  $\sim 700$  and  $1100^\circ\text{C}$ . Introduction of neon led to the onset of oscillation not only at the He I transition, with the laser emission wavelength being  $\lambda = 2.06 \mu\text{m}$ , but also at several transitions of Ne I, emitting radiation in the region of  $\sim 1 \mu\text{m}$ . As the tube was heating up, the lines of oscillation were appearing at different times. The laser lines corresponding to Sr I atoms and Sr II ions were most sensitive to tube heating. The lines of oscillation at transition of He I and transitions of Ne I are marked in the diagram (Fig. 2). The average power of the laser oscillation at the Sr I line with the wavelength  $\lambda = 6.45 \mu\text{m}$  amounted to 40–50% of the total oscillation power in the entire studied range of variation of the GDT discharge channel temperature, reaching  $\sim 4.9$  W. The beginning of the laser oscillation

pulse at the He I line with the wavelength  $\lambda = 2.06 \mu\text{m}$ , as well as that at the Ne I lines at  $\sim 1 \mu\text{m}$ , coincided with the peak of the voltage applied to the GDT (Fig. 1). During oscillation at the Sr I lines near  $3 \mu\text{m}$ , oscillation at the Ne I line with  $\lambda = 585.3$  nm (no. 18 in the table) and a glimpse of oscillation at the Ne I line with wavelength  $\lambda = 540.1$  nm (no. 19 in the table) were also visually observed at the tail of the current pulse.

## ANALYSIS OF RESULTS

The mechanism of inversion at IR transitions of an Sr I atom and Sr II ion has been discussed in detail in [6]. Addition of neon to helium did not influence oscillation at transitions of Sr I and Sr II. However, as we mentioned above, addition of neon to a He + Sr mixture led to laser oscillation at the He I line with the wavelength  $\lambda = 2.06 \mu\text{m}$  and, simultaneously, at a group of lines of Ne in the region near  $1 \mu\text{m}$ . The mixture of helium with neon is known in connection to the invention of the first gas-discharge laser operating at Ne I transitions with wavelengths  $\lambda = 632.8$  and  $\lambda = 1152$  nm ( $1.15 \mu\text{m}$ ), which correspond to transitions from levels  $5s$  and  $4s$  to level  $3p$ , respectively. The relative position of the energy levels of Ne I and He I is shown in Fig. 2. Considering the fact that the pulsed laser action was obtained in the group of Sr I transitions in the vicinity of  $1 \mu\text{m}$ , we turn our attention to the developed multiplet structure of Ne I levels of the  $3p$  configuration, which exhibits a small ( $\Delta E \sim 0.05$ – $0.23$  eV) energy gap between the levels. It is known that, in the case of energy gap  $\Delta E \leq kT_{\text{gas}}$ , populations of multiplet levels in the discharge plasma at average and sufficiently high values of gas pressure become effectively mixed relative to the multiplet center of gravity:

$$E_{\text{cg.}} = (E_1g_1 + E_2g_2 + \dots + E_n g_n) / (g_1 + g_2 + \dots + g_n), \quad (1)$$

where  $g_n$  are the statistical weights of the corresponding levels.

Let us analyze the oscillation conditions at the He I line with wavelength  $\lambda = 2.06 \mu\text{m}$ , Ne I lines near  $1 \mu\text{m}$ , and Ne I line with wavelength  $\lambda = 585.3$  nm in the discharge under consideration.

1. The resonance upper level of the He I transition with wavelength  $\lambda = 2.06 \mu\text{m}$  ( $2p^1P_1$ ) lies high ( $E = 21.22$  eV) and can be efficiently populated by electron impact from the ground state. The presence of the high-energy beam of runaway electrons in the high-voltage discharge [3, 4] and high concentration of helium atoms in the ground state ( $\sim 10^{17} \text{cm}^{-3}$ ) allow exciting the resonance level with high efficiency, whereas the lower metastable level  $2^1S_0$  of He I is populated at a lower rate. Therefore, initially, upon a sharp increase in current before the HSIW front, the so-called self-limited oscillation occurs at the transition

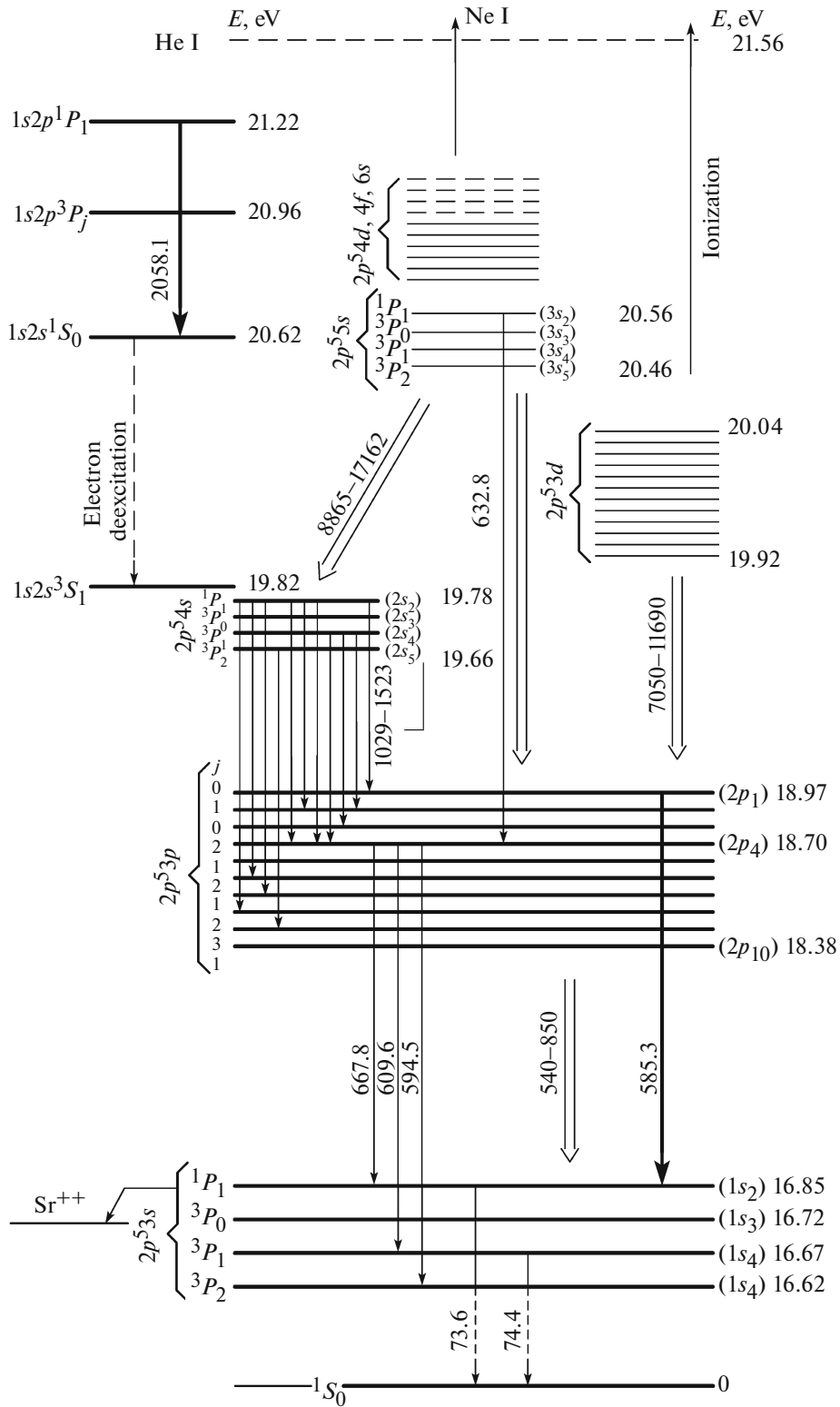


**Fig. 2.** Relative position of energy levels of helium and neon (the ground states of He I and Ne I coincide). Transition wavelengths are given in nm.

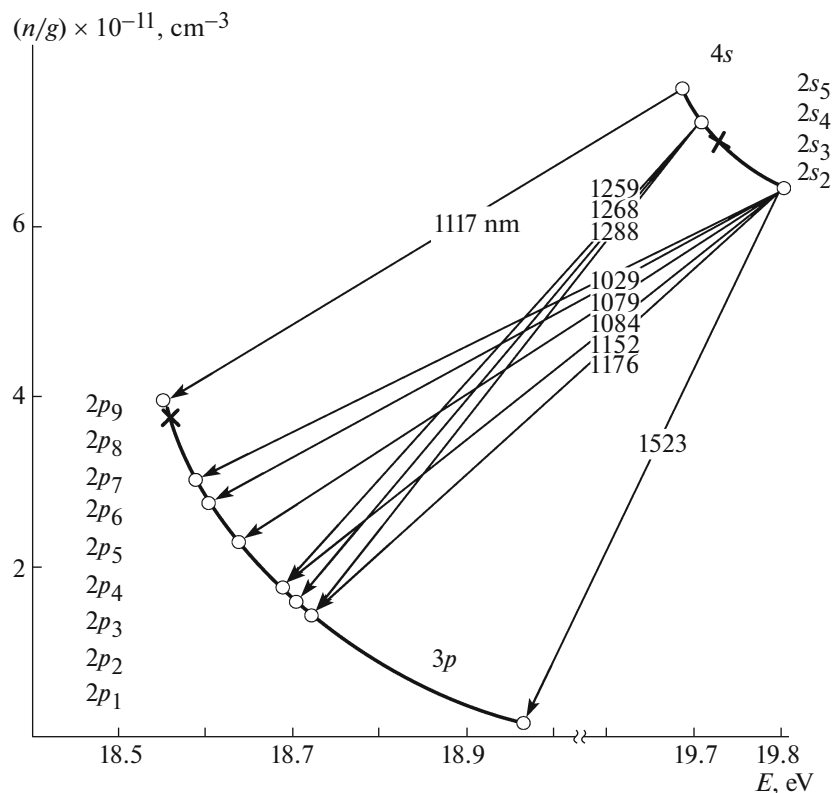


**Fig. 3.** Distribution of populations of  $3p$  and  $4s$  states of Ne in the lasing regime. Crosses denote centers of gravity (expression (1)) of multiplets in a laser based on He + Ne + Sr mixture ( $T_{\text{gas}} \sim 0.3$  eV,  $T_e \sim 4$  eV).

with wavelength  $\lambda = 2.06 \mu\text{m}$ . Subsequent population and depopulation of the levels responsible for laser action at  $\lambda = 2.06 \mu\text{m}$  takes place in plasma induced by runaway electrons behind the HSIW front. In so doing, while the upper (resonance) level remains highly populated due to re-absorption of the resonance radiation, the lower level becomes efficiently depopulated via collisions with electrons and ions under the conditions existing in plasma.

It was shown in [5] that plasma is in a highly ionized state under high voltages realized during breakdown of the discharge gap. Only the highest, with respect to ionization potential, levels of all mixture components are in equilibrium with plasma electrons, and they are depleted to a great extent. At  $T_e \sim 4$  eV,  $n_e \sim 10^{14} \text{ cm}^{-3}$ , upper levels of atoms of all mixture components are highly depleted at  $\Delta E \leq 1.6$  eV (energy is measured relative to the corresponding ionization potentials). Under such conditions, depopulation of the He I  $2^1S_0$  level occurs most efficiently via collisions with free electrons, which drive atoms into the level  $2^3S_1$ . It is known that the effective cross section of this process accompanied by reorientation of spin of the valence electron is large, reaching  $\sim 10^{-14} \text{ cm}^2$ .

2. Ultimately, a sufficiently high population of the  $2^3S_1$  state of He makes possible selective population of

Ne I states of the  $4s$  configuration, which are in resonance with it due to collisions of the second kind with neon atoms in the ground state. Estimates show that, under the conditions of the discussed experiment, the relaxation of the metastable states  $2^3S_1$  of He I occurs within  $\sim 1$  ns as a result of collisions with Ne in the state  $1S_0$ . The Ne I states of the  $4s$  configuration represent the upper laser levels for transitions in Ne in the vicinity of  $1 \mu\text{m}$ . In addition, the  $4s^1P_1$  and  $4s^3P_1$  states of neon atoms are resonance states that can be efficiently populated by absorption of the resonance radiation.

When plasma is in the state of ionization nonequilibrium and the population of upper levels (with  $\Delta E \leq 1.6$  eV) is depleted, the contribution of numerous radiative transitions originating at these levels to the population of Ne I states of the  $3p$  configuration is considerably reduced (Fig. 2). This leads to a strong depletion of the population of Ne I states of the  $3p$  configuration, which represent the lower laser levels for transitions in Ne I in the vicinity of  $1 \mu\text{m}$ .

Formation of the population inversion at  $4s-3p$  transitions in Ne I atoms is illustrated in Fig. 3.

3. Laser oscillation at the yellow line of Ne I at  $\lambda = 585.3 \text{ nm}$  (transition from the  $3p^1S_0$  state to the  $3s^1P_1$  state) was observed in the tail of the current pulse. At

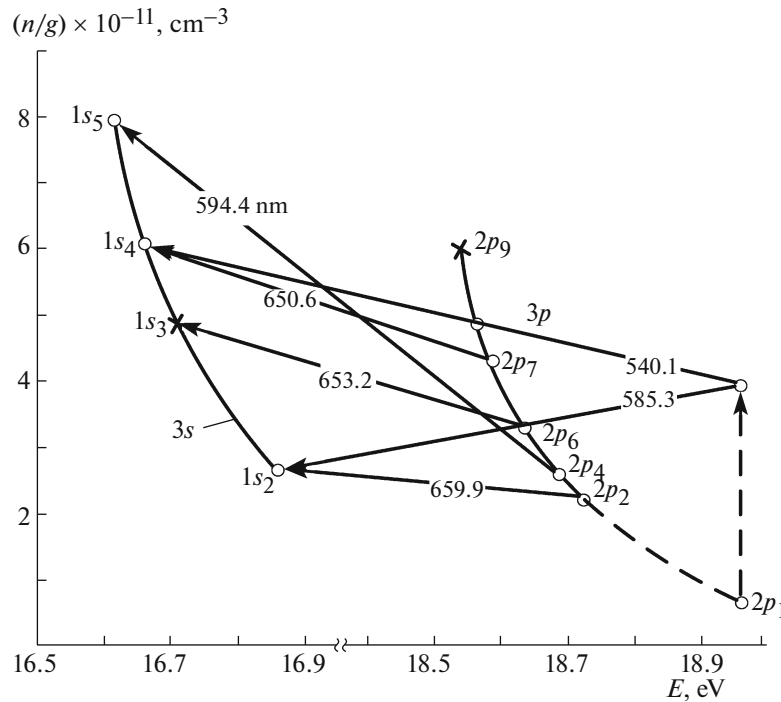
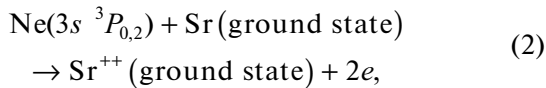


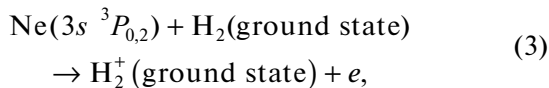
**Fig. 4.** Distribution of populations of  $3p$  and  $3s$  levels of neon in the regime of lasing at transition with a wavelength of  $585.3$  nm in a laser based on He + Ne + Sr mixture ( $T_{\text{gas}} \sim 0.18$  eV,  $T_e \sim 2$  eV).

that time, the plasma experienced a sharp transition from a strongly ionized state to a more equilibrium state, which was accompanied by an efficient population of  $3p$  and  $3s$  states of Ne I due to the radiative flux from upper to lower levels.

As a result, the decay rate of  $3s$  levels of Ne I, including a lower level of the transition with wavelength  $\lambda = 585.3$  nm, considerably increases under collisions with strontium atom in the ground state due to the Penning process. According to [7], the rate of the Penning process in the reaction



is comparable with the rate of the Penning process involving molecular hydrogen,



and is substantial.

Formation of population inversion at laser transitions  $3p-3s$  of neon atoms is illustrated in Fig. 4.

To find the populations of  $3p$  and  $3s$  states of Ne I, we used the results obtained for Ne I transition at the wavelength  $\lambda = 585.3$  nm in the Ne + H<sub>2</sub> mixture in the plasma of another high-voltage-discharge laser [8]. The population inversion at the end of the pulse of current was measured by means of the inverted Rozh-

destvensky hook method. The pressure of neon, the voltage, the conditions for discharge gap breakdown, and the plasma parameters were close to the conditions for obtaining laser action at transition with wavelength  $\lambda = 585.3$  nm in the discussed pulse-periodic laser based on He + Ne + Sr mixture. Comparing expressions (2) and (3), we note that smaller amount of Sr atoms (ground state) compared to H<sub>2</sub> (ground state) is compensated by more efficient population of Ne I energy levels ( $3s \ ^3P_{0,2}$ ) in He + Ne + Sr mixture due to additional radiative flux. The validity of using results of [8] for estimating the absolute values of populations is further justified by the fact that average output powers at the laser transition in Ne I with wavelength  $\lambda = 585.3$  nm are comparable in both discharges. Population inversion at Ne I transition with wavelength  $\lambda = 585.3$  nm appears due to the fact that, at  $kT_{\text{gas}} < \Delta E$  ( $\Delta E$  is the difference of energies of states  $2p_1$  and  $2p_2$ ), state  $2p_1$  is not subjected to distribution of populations between multiplet level with a distribution function determined by the gas temperature, but is populated with respect to the center of gravity of the  $3p$  multiplet with a distribution function determined by electron temperature  $T_e$  (Fig. 4). Taking into account the above arguments, we note that the data on absolute values of level populations should be considered as estimates.

## CONCLUSIONS

The He + Ne + Sr mixture is a medium enabling multiple-wavelength laser oscillation under excitation in a pulsed high-voltage discharge. During the current pulse, high-frequency collisions between atoms and between ions and atoms, as well as collisions between electrons and atoms, influence the population of the upper and lower laser levels. The high pulse repetition rate affords high laser output power.

The conducted investigation showed that electric current in the considered discharges exhibits two stages (Fig. 1). At the first stage, the discharge current is low and is mainly determined by the distributed capacitance [2, 3]. At the second stage, the current sharply increases. Comparison of  $I(t)$  and  $V(t)$  dependences with spatiotemporal variation of plasma parameters [5] shows that a sharp increase in the current and peak voltage across the GDT coincides in time with a sharp increase in the concentration of electrons and the peak of their temperature. At this moment, plasma is located at a considerable distance from the GDT walls and keeps moving toward the center, changing its parameters while retaining some degree of ionization that is nonequilibrium until termination of the current pulse.

Recently, observation of simultaneous multiple-wavelength laser oscillation in a He + Ne + Sr mixture both during the current pulse ( $\lambda = 6.45, 3.06, 3.01, 2.92, 2.69, 2.60, 1.09, \text{ and } 1.03 \mu\text{m}$ ) and  $\sim 200$  ns after its termination ( $\lambda = 0.430 \mu\text{m}$ ) was reported in [9]. All the listed laser lines (in the IR spectral region) belong to Sr I atoms and Sr II ions (see table). The laser emission line at  $\lambda = 0.430 \mu\text{m}$  (in the visible spectral region) belongs to Sr II ions. The voltage across the GDT, gas mixture pressure, and length of the discharge tube were varied, while the inner tube diameter of 2.7 cm was kept unchanged. The construction of the

pulse-periodic high-voltage discharge laser and the scheme of its electric circuit were the same as in [2].

The results obtained in [2, 5, 6, 9] and in the present work illustrate the possibility of achieving simultaneous multiple-wavelength laser oscillation at several transitions in the infrared and visible spectral regions in a high-voltage pulse-periodic longitudinal-discharge laser based on a He + Ne + Sr mixture. The wavelength distribution of the laser emission can be varied by changing the external parameters of the discharge (and, thus, plasma parameters) without changing basic construction of the pulse-periodic metal vapor laser and its associated electric circuit.

## REFERENCES

1. A. N. Soldatov, A. G. Filonov, A. S. Shumeiko, et al., Proc. SPIE—Int. Soc. Opt. Eng. **5483**, 252 (2004).
2. A. N. Soldatov, N. A. Yudin, Yu. P. Polunin, et al., Izv. Vyssh. Uchebn. Zaved., Ser. Fiz. **51** (1), 6 (2008).
3. L. M. Vasilyak, S. V. Kostyuchenko, N. N. Kudryavtsev, and I. V. Filyugin, Usp. Fiz. Nauk **164** (3), 263 (1994).
4. A. N. Tkachev and S. I. Yakovlenko, JETP Lett. **77**, 221 (2003).
5. T. M. Gorbunova, A. N. Soldatov, and A. G. Filonov, Izv. Vyssh. Uchebn. Zaved., Ser. Fiz. **54** (3), 55 (2011).
6. T. M. Gorbunova, A. N. Soldatov, and A. G. Filonov, Opt. Atm. Okeana **17** (2–3), 262 (2004).
7. A. M. Boichenko, V. I. Derzhiev, A. G. Zhidkov, et al., Tr. Inst. Obshch. Fiz., Ross. Akad. Nauk **21**, 44 (1989).
8. T. M. Gorbunova, Yu. P. Mikhailichenko, and A. M. Yancharina, Izv. Vyssh. Uchebn. Zaved., Ser. Fiz. **37** (12), 3 (1994).
9. A. N. Soldatov, S. Yu. Mirza, Yu. P. Polunin, and A. S. Shumeiko, Izv. Vyssh. Uchebn. Zaved., Ser. Fiz. **56** (11), 6 (2013).